3D segmentation of the airway tree using a morphology based method

Benjamin Irving, Paul Taylor, and Andrew Todd-Pokropek

University College London, WC1E 6BT, UK,
b.irving@ucl.ac.uk

Abstract. Segmentation of the airways is useful for the analysis of airway compression and obstruction caused by pathology. This paper outlines an automatic method for segmentation of the airway tree. This method includes algorithms to detect the trachea, segment the trachea and main bronchi by thresholding and region growing, and segment the remaining bronchi by morphological filtering and reconstruction. Morphological filtering and reconstruction are applied to all slices in the axial, sagittal and coronal planes and are used to extract the smaller airways. Bounded space dilation with a leak removal restriction is applied as a region growing method. This method was evaluated on 20 cases as part of the MICCAI pulmonary image analysis workshop. The mean number of branches detected as a percentage of possible branches was 43.5%, the mean tree length detected as a percentage of the entire tree length was 36.4% and the false positive rate – that is, the percentage of the total volume that was incorrectly segmented – was 1.27%

1   Introduction

This paper outlines a morphology based algorithm for the segmentation of the airways in three dimensions from computed tomography (CT) images. The aim was to develop a flexible method for extraction of the airways from CT images. This tool will be required to model airway changes in paediatric patients with pulmonary tuberculosis leading to compression and deformation of the airways. A morphology based airway segmentation method was chosen. This method was applied to adult patients for the MICCAI pulmonary image analysis workshop and, therefore, adult patients are the focus of this report.

This method further develops the use of morphological reconstruction to extract the airways reported previously by Aykac et al [1] and Pisupati et al [2]. Both Aykac et al and Pisupati et al perform greyscale morphological reconstruction on each CT slice to extract the regional minima and, therefore, enhance the airways (discussed in Section 2.3). The greyscale morphological reconstruction is applied to each slice using a range of marker images that have been created from greyscale closing the original image with a range of structuring elements (SE). The SEs are chosen to be a similar size to the cross section of the airways present in the slice in order to enhance them. The reconstructed image is

subtracted from the original image and a threshold is applied. 2D seeded region growing is then applied slice by slice to extract the airways from the binary volume [1, 2]. Pisupati et al [2] applied their method to CT images of canine lungs while Aykac et al [1] applied their method to CT images of human lungs.

Morphology based methods have also been applied by Preteux et al [3] and Fetita et al [4]. Fetita et al [4] use an algorithm that calculates the connection cost between points in an image – that is, the smallest threshold that will provide a binary path between two points – to enhance the airways in CT slices. Once enhanced, the images are not thresholded and 3D reconstruction is performed on the greyscale images using a local energy minimisation algorithm. This energy function takes into account the tree topology of the airways as well as the greyscale intensity. There are a number of other non-morphology based methods have been used to segment the airways.

This study uses a similar morphology based method to that of Aykac et al [1] and Pisupati et al [2]. These methods have, however, been extended with the aim of improving segmentation of smaller airways and airways parallel to the slice, as well as reducing leaks. The extensions include three dimensional morphological filtering and leak removal using 3D dilation. The following section discusses the segmentation algorithm, which includes an initialisation step, a step to extract the trachea and main bronchi, a step to extract the smaller airways using morphology, and finally a region growing and leak removal step.

2   Methods

An overview of the algorithm is shown in figure 1. Note that thresholding and seeded region growing is used to segment the trachea and left and right main bronchi. It is possible to use morphology based segmentation – the method used for the rest of the segmentation – for the larger branches as well, however, this means larger structuring elements (SE), increasing the likelihood that areas of the lung with a circular appearance will be segmented.

2.1   Initialisation

This method requires an initialisation point at the start of the trachea. To select this point automatically, the slices are orientated using the DICOM header information and the lung boundaries are roughly segmented by thresholding for air regions in the coronal plane through the centre of the patient. Air filled regions were classified as regions below -500 HU. Certain cases did not conform to the HU scale and, therefore, if the slice contained only values above -500 HU then the threshold was set to *MinVal+500*. In this algorithm 10 slices above the upper most point of the segmented lung region was chosen as the starting axial slice for the segmentation. This step is included because the large variation in the region covered by a CT scan, makes it difficult to select an appropriate starting slice without knowing the location of the lung fields. After an axial slice has been selected, the trachea is found in that slice by applying a threshold to identify air
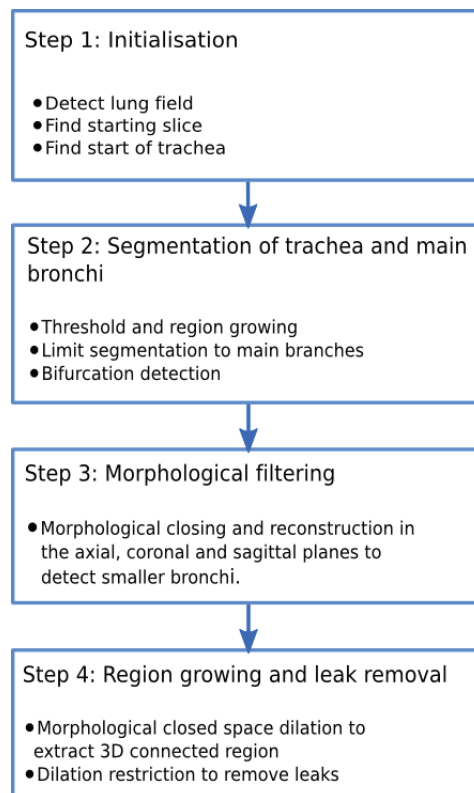
Step 1: Initialisation

- Detect lung field
- Find starting slice
- Find start of trachea

Step 2: Segmentation of trachea and main bronchi

- Threshold and region growing
- Limit segmentation to main branches
- Bifurcation detection

Step 3: Morphological filtering

- Morphological closing and reconstruction in the axial, coronal and sagittal planes to detect smaller bronchi.

Step 4: Region growing and leak removal

- Morphological closed space dilation to extract 3D connected region
- Dilation restriction to remove leaks

Fig. 1. Outline of algorithm to segment the airway tree

filled regions. The trachea is detected by comparing the possible regions in terms of position, size and compactness in a similar way to that of Aykac et al [1] and Mori et al [5]. The area parameter was calculated as the area of the object once the optimal area – chosen to be 400 pixels – was subtracted. The position of the object was defined as the euclidean distance from the ideal position – which was chosen to be (200, 256). Compactness (C) was calculated from perimeter (P) and area (A) as $C = \frac{P^2}{A}$. The segmentation of the starting slice is used as a seed for the rest of the segmentation.

2.2   Segmentation of Trachea and Main Bronchi

Thresholding and region growing are applied to the axial slices using the segmentation from the previous slice as seed points. This is applied progressively to each slice from the start of the trachea.

Greyscale thresholding is used only to segment larger branches, because if smaller branches are included in the segmentation, the similar greyscale intensities of the small bronchi and lungs will cause leaking into the lungs. Therefore, for each step, the newly segmented region is evaluated and steps are taken to stop the segmentation of smaller vessels. If the segmented region is more than double the area of the previous slice then a leak is considered to have occurred through smaller bronchi into the lungs. This leak is excluded by finding the centre-of-mass (CM) and the maximum radius of the segmented region in the previous slice, and iteratively reducing the radius and recalculating the CM until a specified compactness is reached; this is used to restrict the segmentation of the current slice (see figure 2).

The position of the bifurcation of the trachea and main bronchi is estimated by labelling the number of connected regions in each slice that have been seeded by one connected region in the previous slice. If two separate regions are seeded by one connected region in the previous slice then bifurcation is considered to have occurred. When the trachea bifurcates, each of the main bronchi are followed and when the main bronchi bifurcate then the procedure is stopped.

2.3   Morphological Filtering

To detect bronchi beyond the main bronchi, morphological greyscale reconstruction is applied to all CT slices to extract local minima and, therefore, enhance the airways.

Greyscale reconstruction is an extension of binary reconstruction. Binary reconstruction is the application of successive dilations within objects of a binary image as shown below [6, 7]:

$$\rho_B(X) = \lim_{n \to +\infty} \delta_B^{(n)}(X) \tag{1}$$

where $\delta_B^{(1)}(X) = (X \oplus K) \bigcap B$ and $\delta_B^{(n)}(X) = \delta_B \circ \delta_B \circ ... \delta_B(X)$ for n times, and the marker (X) is a subset of the mask (B). The marker (X) is made up of seed
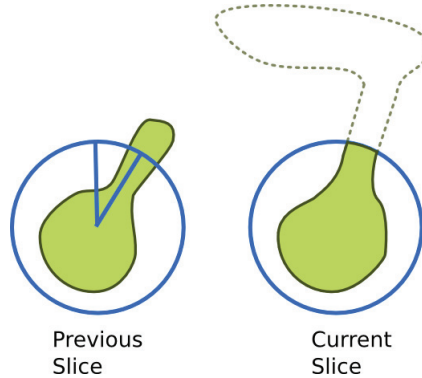
Previous
Slice

Current
Slice

Fig. 2. Excluding leaks in trachea and main bronchi segmentation by reducing the radius and recalculating the CM iteratively until a specified compactness is reached

points – that is, where the dilation starts in the object. The mask is generally the image that is being operated on [6, 7]. K is a SE used in the dilation and $\oplus$ is the dilation operator.

This definition is expanded for greyscale reconstruction [6, 7]. A marker and mask image are used where every pixel in the marker image has a pixel intensity less than or equal to the intensity of the corresponding pixel in the mask image. The marker and mask images are then thresholded over a range of thresholds and binary reconstruction is performed on each threshold. The maximum pixel intensities of the binary reconstructed images form the greyscale reconstructed image. With a good choice of a marker image this method can be used to create a reconstructed image with the intensity peaks removed. This can then be subtracted from the original image to enhance the peaks. Figure 3 is an illustration of greyscale reconstruction in 1 dimension and shows the Mask and Marker greyscale values. The reconstructed image is represented by the shaded area.

In this study, the greyscale closing of the image of interest is used as the marker image, as shown below, in a similar way to that of Aykac et al[1] and Pisupati et al [2]:

$$X = B \bullet D = (B \oplus D) \ominus D \qquad (2)$$

where X is the marker image, B is the original image (used in reconstruction as the mask image) and D is the SE. D will control the shape of the marker image and, therefore, which airways are enhanced in the reconstruction, since the difference between the original image and the reconstructed image gives
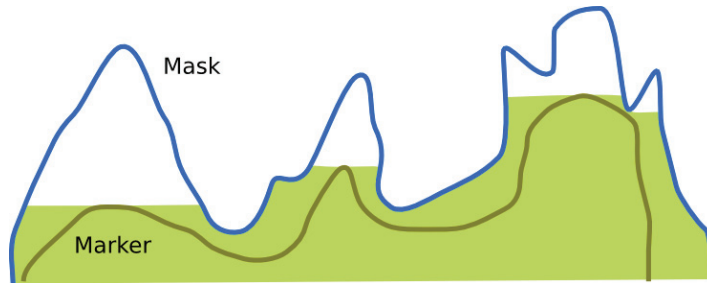
Fig. 3. Greyscale reconstruction

an airway enhanced image. Applying morphological reconstruction a number of times to a slice using different SE sizes to produce marker images will enhance airways of different cross sections [1, 2]. Therefore, morphological reconstruction was applied using marker images produced using a range of SEs. The smallest SE chosen in this study is a 4-connected binary SE. Larger SEs are created by applying successive dilations to the smallest SE i.e. $D_n = D \oplus D \oplus ... \oplus D$ n times. The number of dilations used to create the largest SE for filtering the axial, coronal and sagittal slices were set to 12, 6 and 6 respectively. Therefore, for each slice in each orientation SEs from a 4-connected binary SE to an SE after 6 or 12 dilations are used to generate marker images.

As described earlier, reconstruction is applied to the range of marker images for each slice. Each reconstructed image is subtracted from the original image to enhance airways. These subtracted images are thresholded and the union of the thresholded images provides a binary slice with all possible airway locations. The threshold fraction used for the axial, coronal and sagittal slices were set to 0.3, 0.4 and 0.4 respectively. The threshold value is obtained from this threshold fraction in terms of the minimum and maximum greyscale values in the reconstructed slice i.e. $ThreshValue = ThreshFrac * (MaxPixelValue - MinPixelValue) + MinPixelValue$. Morphological filtering was applied slice by slice to the volume.

Aykac et al [1] and Pisupati [2] applied the filtering to each axial slice. We apply 3D filtering i.e. to each slice in the axial, coronal and sagittal plane. This is because of poor detection of branches parallel to the slice if just one direction is used. The axial plane is filtered last in order to enhance segmentation of bifurcation areas that can appear large and non circular from the axial plane if branches are parallel to the slice. Smaller branches parallel to the axial plane are, therefore, segmented first leaving more circular bifurcation areas that are detected with the axial filter (see figure 4).
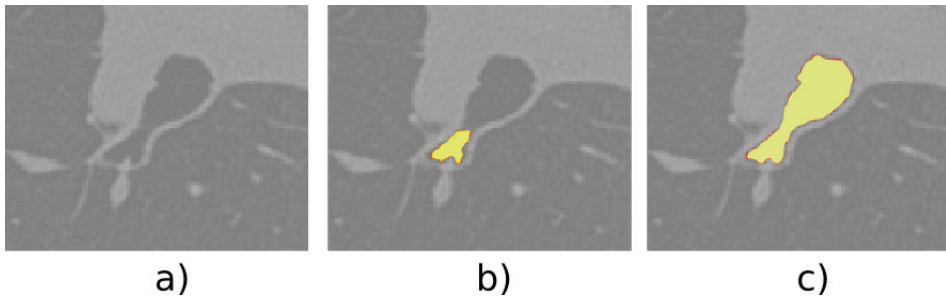
Fig. 4. Using 3D filtering to segment objects that are non-circular in the axial plane. a) Unsegmented section of the airway tree. b) Parallel vessels segmented using coronal and sagittal filtering. c) Axial filtering applied.

2.4   Region Growing and Leak Removal

Once possible regions have been detected using morphological filtering and reconstruction, bounded space dilation is applied to the binary volume as a region growing technique from the initial seed point [8].

Closed space dilation is particularly useful because airway branching can be monitored while the region growing is taking place. Closed space dilation is described as follows [8]:

$$X \oplus_B K = X_N = (X_{N-1} \oplus K) \bigcap B = ...$$ (3)

where $X = X_0$ is the initial seed, B is the region being segmented, K is the kernel and $\oplus$ is the morphological dilation operation [8]. Closed space dilation acts like the dilation operator except it is restricted to the shape of the object B.

This method is seeded by the initial slice in the trachea, and 3D closed space dilation is applied until the segmentation volume does not increase using a $3 \times 3 \times 3$ SE. 2D closed space dilation, which is used previously [1], is applied to each slice individually and requires a number of forward and backward passes through the whole volume to capture the 3D data. While 3D dilation allows any complexity of topology to be followed, we specify a constraint that the object remains 6-connected.

In some cases other objects that are of a similar size and shape to that of the airways are enhanced by the morphological reconstruction and remain when thresholded. If after thresholding, the object is 6-connected to the airway region it will be segmented; this causes leaks. Leaking is prevented by applying

a restriction on the dilation. The change in cross section of each branch can be monitored by calculating the area of the "growth front" of each branch, where the growth front is the area added to the connected region for each iteration of the closed space dilation [8]. The growth front of each branch is calculated by labelling in 3D each connected object of the growth front and labelling the connected growth front from the previous step. To detect leakage where the volume increase substantially, the volume of the last 3 dilations for each branch are compared to the 3 dilations before that. If the ratio of the volumes is above a specified threshold of double the size then closed space dilation along this branch is stopped.

3   Results

Figure 5 shows an example airway segmentation (visualised using ITK-SNAP). The algorithm parameters were adjusted using the 20 training images and these parameters were fixed for the 20 test images. The segmentations of the test images were submitted to EXACT09 for analysis. A ground truth was established by the organisers by taking the union of all the correct branches from all the submissions. Each submission was then compared to this ground truth. Table 1 shows the accuracy of the algorithm for the 20 test cases provided. The meaning of each heading is as follows: *branch count* is the number of branches detected correctly, *branch detected* is the proportion of branches detected compared to the ground truth, *tree length* is the sum of all correctly detected branches, *tree length detected* is the tree length compared to the ground truth, *leakage count* is the number of correct regions bordering incorrect regions, *leakage volume* is the volume of regions wrongly detected, and *false positive rate* is the fraction of wrongly detected regions out of all detected regions. This algorithm produced a fair result; the mean number of branches detected was 43.5%, the tree length detected was 36.4% and the number of false positives was 1.27%. The time taken to process a case varied according to computer specifications and the number of slices containing airways. The mean and standard deviation of the time taken to complete each of the 20 cases was 71 ± 18 minutes using a single core of a quad core 2.83GHz system. This time can be considerably decreased by converting the code from Matlab to C or another compiled language.

4   Discussion

This paper discusses a method to segment the airways using morphological closing and reconstruction developed in previous studies [1, 2]. The algorithm discussed in this paper further develops these methods to detect smaller branches and reduce leaking. This is done by applying the filtering in 3D using thresholds and structuring elements optimised for each direction, a thresholding and region growing method is applied to the larger branches to reduce the required range of structuring elements and 3D bounded space dilation along with individual branch volume change monitoring to remove additional leaks.

Table 1. Evaluation measures for the twenty cases in the test set.

|	Branch count	Branch detected (%)	Tree length (cm)	Tree length detected (%)	Leakage count	Leakage volume (mm^3)	False positive rate (%)
CASE21	101	50.8	55.7	50.4	0	0.0	0.00
CASE22	76	19.6	48.4	14.7	0	0.0	0.00
CASE23	33	11.6	23.9	9.2	0	0.0	0.00
CASE24	86	46.2	63.4	39.0	0	0.0	0.00
CASE25	123	52.6	91.4	36.3	3	11.6	0.06
CASE26	55	68.8	37.8	57.5	9	16.4	0.23
CASE27	83	82.2	55.6	68.7	2	95.2	1.01
CASE28	79	64.2	58.4	53.3	7	121.3	1.34
CASE29	92	50.0	62.6	45.4	3	17.9	0.19
CASE30	94	48.2	66.6	43.6	2	48.2	0.51
CASE31	91	42.5	59.0	33.6	4	1487.4	11.71
CASE32	45	19.3	35.8	16.5	5	803.2	6.94
CASE33	85	50.6	59.6	40.5	0	0.0	0.00
CASE34	140	30.6	90.3	25.2	3	32.4	0.17
CASE35	82	23.8	53.8	17.4	0	0.0	0.00
CASE36	148	40.7	147.0	35.7	1	1.9	0.01
CASE37	65	35.1	46.9	26.4	1	94.5	0.76
CASE38	73	74.5	44.1	66.3	4	57.5	0.65
CASE39	155	29.8	111.0	27.1	1	1.4	0.01
CASE40	116	29.8	80.7	20.9	5	256.1	1.71
Mean	91.1	43.5	64.6	36.4	2.5	152.3	1.27
Std. dev.	32.3	19.1	28.2	17.1	2.6	362.7	2.91
Min	33	11.6	23.9	9.2	0	0.0	0.00
1st quartile	73	29.8	46.9	20.9	0	0.0	0.00
Median	86	44.4	58.7	36.0	2	17.1	0.18
3rd quartile	123	64.2	90.3	53.3	5	121.3	1.34
Max	155	82.2	147.0	68.7	9	1487.4	11.71
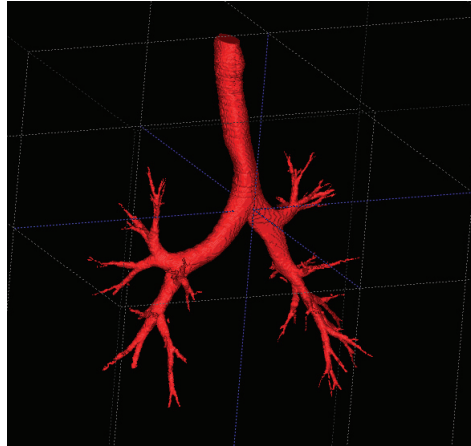
Fig. 5. Segmentation of the airways of CASE02

This method was developed for the segmentation of the airways in paediatric patients and will be used in the modelling and detection of airway deformation and stenosis. The paediatric images are of a poorer quality due to the smaller patient sizes and, therefore, fewer airway branches are visible. This algorithm could be optimised for adult airways in order to obtain better results. Branch detection will be improved by including branches that are not 6-connected to the main airway tree because of small areas of poor morphological segmentation due to airway wall discontinuities. Small discontinuities in the segmentation for CASE 22, 23, 32 and 35 removed a number of large branches when region growing was applied leading to poorer results. A more sophisticated region growing method would correct this. The benefit of this method is the low false positive rate. This is required for paediatric TB cases because exudate in the lungs increases the likelihood of segmentation leaks. Exceptions are CASE31 and CASE32 that have relatively high leakage. A further development of this method for paediatric airways includes detection of disconnected airway branches due to complete obstruction of the airways due to pathology.

References

1. Aykac, D., Hoffman, E., McLennan, G., Reinhardt, J.: Segmentation and analysis of the human airway tree from three-dimensional X-ray CT images. Medical Imaging, IEEE Transactions on **22** (2003) 940–950
2. Pisupati, C., Wolff, L., Mitzner, W., Zerhouni, E.: Segmentation of 3D pulmonary trees using mathematical morphology. Mathematical morphology and its applications to image and signal processing. Atlanta, Ga: Kluwer Academic Publishers (1996) 409–416
3. Prêteux, F., Fetita, C., Capderou, A., Grenier, P.: Modeling, segmentation, and caliber estimation of bronchi in high resolution computerized tomography. Journal of Electronic Imaging **8** (1999) 36–45
4. Fetita, C., Preteux, F., Beigelman-Aubry, C., Grenier, P.: Pulmonary Airways: 3-D Reconstruction From Multislice CT and Clinical Investigation. IEEE Transactions on Medical Imaging **23** (2004) 1353–1364
5. Mori, K., Hasegawa, J., Toriwaki, J., Anno, H., Katada, K.: Recognition of Bronchus in Three-Dimensional X-ray CT Images with Application to Virtualized Bronchoscopy System. Proceedings of ICPR **3** (1996) 528–532
6. Vincent, L.: Morphological grayscale reconstruction in image analysis: applications and efficient algorithms. Image Processing, IEEE Transactions on **2** (1993) 176–201
7. Vincent, L.: Morphological grayscale reconstruction: definition, efficient algorithm and applications in image analysis. In: Proceedings of Computer Vision and Pattern Recognition. Volume 92. (1992) 633–635
8. Masutani, Y., Schiemann, T., Hoehne, K.: Vascular Shape Segmentation and Structure Extraction Using a Shape-Based Region-Growing Model. Lecture notes in computer science (1998) 1242–1249